

RIJKSUNIVERSITEIT GRONINGEN

BACHELOR THESIS

A Deeper look at the Anomalous Globular Cluster Luminosity Function of
NGC-1052 DF2



rijksuniversiteit
groningen

Author:
J.F. Lania

Supervisors:
R. F. Peletier
T. Saifollahi

Abstract

We present a photometric analysis of the globular clusters of NGC-1052 DF2 (DF2). DF2 is an ultra diffuse galaxy which appears to have a negligible dark matter content and overly bright globular clusters; the Globular Cluster Luminosity Function (GCLF) seems to peak at $M_V = -9$ instead of the nigh-universal value of $M_V = -7.5$. A previous study observed a secondary peak around the canonical value. In this work, we used SExtractor software to extract sources upon which we perform a photometric selection and statistical background subtraction using extremely deep HST data, thereby obtaining the GCLF of DF2's globular clusters. We observe no evidence of bimodality in the GCLF, and a reduced χ^2 test shows that the data favours a single mode Gaussian over a bimodal model, although neither model provides a good fit.

Contents

1 Introduction	2
2 Analysis	4
2.1 Data	4
2.2 Source Extractor	4
2.3 Photometric selection	6
2.4 Errors	8
2.5 Apertures	9
3 Results	11
3.1 Luminosity Functions	11
3.2 Gaussian modeling	14
4 Discussion	14
5 Conclusion	16
6 References	17
7 Appendix: Python Code	19

1 Introduction

Since the 1980's, a number of low surface-brightness galaxies have been discovered in well-studied galaxy clusters, such as the Fornax and Virgo clusters (Saifollahi (2022), Binggeli et al. (1985)). The detection of these galaxies is limited due to their intrinsic low luminosities, however new deep sky optical surveys have contributed to their field of study. As such, study in the field of low surface-brightness galaxies is becoming more active (Román et al., 2021).

A subclass of low surface brightness galaxies are the so-called Ultra Diffuse Galaxies, or UDGs (van Dokkum et al., 2015). These galaxies appear to have extreme amounts of dark matter in both senses of the term. UDG NGC-1052 DF44 was proposed by Dokkum et al. (2016) and van Dokkum et al. (2017) to have a dark matter fraction within its half-light radius of approximately 98 %, and a dark matter halo mass of order $M_{halo} \approx 10^{11} M_{\odot}$; though this was shown to be erroneous by Saifollahi (2022). Conversely, other UDGs appear to have little to no dark matter at all. One such dark matter deficient galaxy, NGC-1052 DF2, has been extensively studied in the past years, with at least 40 publication regarding it in the last five years; those by Shen et al. (2021b), van Dokkum et al. (2018b), Trujillo et al. (2019) and Shin et al. (2020) constituting some examples over this time. NGC-1052 DF2, hereafter referred to simply as DF2, is a UDG thought to be associated with the NGC-1052 galaxy group. Though it had been identified as belonging to this group by wide-image surveys of the NGC-1052 cluster beforehand, in 2018 a deeper study of the galaxy was carried out and concluded that the galaxy has a halo to luminous ratio M_{halo}/M_{stars} of order unity, indicating that it possesses little to no dark matter (van Dokkum et al., 2018b).

Additionally, several globular clusters were identified thought to be associated with DF2. While it is not uncommon for galaxies such as DF2 to have a globular cluster system, the luminosities of these globular clusters appear to be anomalous (van Dokkum et al., 2018a). Many identified globular cluster systems adhere to a canonical globular cluster luminosity function

(GCLF), which is approximately Gaussian in shape and has an absolute peak magnitude of approximately -7.5 . This GCLF is nigh-universal (Rejkuba, 2012), which facilitates the use of the canonical GCLF as a standard candle for the purposes of distance measurements: see Beasley (2020) and Harris (1991) for more information. However, the globular cluster system of DF2 has been suggested to have a GCLF with a narrow peak value -9.1 , approximately 4.4 times brighter than the canonical value, as presented in van Dokkum et al. (2018a). Combined with its puzzling dark matter content, it would seem that DF2 challenges several previous assumptions regarding galaxy formation models. In addition, a galaxy apparently similar to DF2 was discovered in 2019 by the same research group, named NGC-1052 DF4, raising the possibility that galaxies with these interesting features may not be as uncommon as thought (van Dokkum et al., 2019).

Research into DF2 and these particular anomalies has been ongoing since the papers by Van Dokkum were published. It is interesting to note that both the abnormally bright globular cluster luminosities and the dark matter content are distance-dependant properties: a larger distance shifts the peak of the GCLF to brighter absolute magnitudes. At a further distance, the stellar mass of the galaxy (inferred through a mass-luminosity relation) would appear to be higher, leaving less room for dark matter content. One study by Trujillo et al. (2019) pointed at these facts, and estimated a distance of 13.4 ± 1.14 Mpc using a variety of distance measurements. In contrast, Van Dokkum 2018 estimated DF2 to have a similar distance as the closest massive galaxy (NGC-1052), giving an estimate of 20 Mpc. Under the distance measurement by Trujillo et al. (2019), the galaxy appears far more ordinary: it has a significant dark matter fraction and has comparatively normal globular clusters in terms of luminosity and size. Some time later, a paper by Shen et al. (2021a) measured the distance to DF2 using the Tip of the Red Giant Branch method, this time finding a distance of 22.1 ± 1.2 Mpc - a distance under which the anomalies would be even more extreme. A two-way debate has begun to form, with proponents of a closer distance of 13.4 Mpc and those in favour of a distance of 20 Mpc. As of today, the true distance to DF2 remains in dispute.

The anomalies in DF2 pose interesting questions for several models of galaxy formation and dark matter paradigms. Dark matter has long been considered pivotal to the formation of galaxies, as they are thought to form when clumps of dark matter interact with baryonic matter. In a scenario without dark matter, stars would likely not organise themselves in a collection as we see in galaxies, but be spread more diffusely across space. DF2 would demonstrate that dark matter is not always present in galaxies, which is itself an argument for its existence as dark matter may be a 'substance' that is often, but not always, found in galaxies. As pointed out by van Dokkum et al. (2018b), DF2 also could falsify alternative theories to dark matter which would expect a trace of it to be found in every galaxy. Supposing that dark matter deficient galaxies exist, Silk (2019) put forwards that current galaxy formation models struggle to explain their origins. In order to examine what the existence of DF2 will mean for cosmology and astronomy as a whole, its distance must be pinned down to an agreed upon value.

Several theories and studies have examined the formation of dark matter deficient galaxies such as DF2. A study by Ogiya et al. (2021) examined the possibility that such galaxies can result from tidal stripping, and if it is possible for a galaxy thus formed to have bright globular clusters like DF2 does. The study shows that it is possible for DF2 to have formed this way, though another study by Müller et al. (2019) reports no evidence of any recent tidal interaction in either DF2 or DF4. This appears to be corroborated by Montes et al. (2021). Other studies are investigating the possibility that galaxies such as DF2 form from collisions of gas-rich dwarf galaxies. In such scenarios, a high-velocity collision may cause the dark matter to be separated

from the warm disc gas, which is compressed to form stars. (Shin et al., 2020). A third possibility is that they are dwarf galaxies that formed in large gas clouds, which was then stripped away by luminous quasars or interactions with other galaxies (Duc et al., 2014).

Recently, a paper by Shen et al. (2021b) revisited the GCLFs of DF2 and DF4 and corroborated the earlier findings regarding the anomalous GCLFs of these galaxies. Additionally, the study claims to have found a sub-population of less luminous globular clusters, forming a small 'second peak' in the GCLF around the canonical value. Now, using HST data that is nearly twenty times deeper than the data used by previous studies, this thesis aims to revisit DF2, photometrically identify its globular clusters and examine their luminosity function. In particular, we aim to investigate more closely the claimed sub-population of globular clusters around the canonical value. To perform a direct comparison with the works of Shen et al. (2021b), we will follow the methodology of their study rather closely. In section 2 of this thesis, this methodology will be discussed in detail. In section 3, the results of the analysis will be presented. In section 4, we will discuss the accuracy and validity of the analysis and the results. We summarize and conclude the paper in section 5.

2 Analysis

2.1 Data

The data consists of a total of 38 exposures of the Hubble Space Telescope's Advanced Camera for Surveys (ACS) taken in late 2020. The data comprises 19 exposures of 2020 seconds each in the V_{606} filter, and 19 exposures of approximately 2080 seconds in the I_{814} filter. Barbara (2019) The exposures were stacked and converted to a FITS format to be used in the analysis, with data reduction on them being performed using AstroDrizzle. This process was carried out by a team at the IAC ¹. The data reduction itself will not be covered in this paper.

Each .fits file contains two frames; a SCI frame containing science-ready data and a weight map setting the priority of each pixel. The V_{606} filter is slightly smaller than the other filter, comprising a stacked image of 6445x6826 pixels versus 8639x8455 pixels for the I_{814} filter. The data is expected to be complete up to 28 mags, since it is deeper than the data used by Saifollahi (2022), which used fewer orbits of data. The paper by Shen et al. (2021b) used two orbits (1 in V_{606} , 1 in I_{814}) for their analysis of DF2 as opposed to the 38 orbits used in this analysis.

2.2 Source Extractor

The data was analyzed using Source Extractor software (SExtractor), with the aim of identifying globular clusters using photometry. Separate configuration files were made for the two filters, with the main differences between them being the weight maps, photometric zeropoints and background values. The photometric zeropoints for each filter were obtained using a web-based zeropoint calculator for the ACS by supplying the date of observations and the desired filter, leading to values of $M_0 = 26.486$ for V_{606} and 25.935 for I_{814} . Background values were initially computed using a simple python script, by forming a histogram of pixel photon counts and taking the median as an approximation for the background value. The values obtained through this routine were $B_g = 1.05 \cdot 10^{-3}$, $8.12 \cdot 10^{-4}$ for V_{606} and I_{814} respectively. SExtractor automatic background computation was however used for the majority of the analysis, using a BACK_SIZE parameter of 128.

¹Instituto de Astrofísica de Canarias (Institute of Astrophysics of the Canary Islands)

Apart from these differences, the configuration files for each filter were kept identical. In order to optimize SExtractor, the program was run over both filters numerous times while varying the parameters slightly during each iteration. The results were inspected graphically using Aladin graphical software. Aperture images, showing the extracted sources and the aperture in which SExtractor performs photometry, were inspected after each iteration in order to examine whether apparent sources within the image were extracted correctly. After optimizing the program in this way, the following parameters values were used:

- DETECT_MINAREA = 4
- DETECT_THRESH = 1.5
- ANALYSIS_THRESH = 1.5
- DEBLEND_NTHRESH = 16
- DEBLEND_MINCONT = 0.0005
- PHOT_APERTURES = 5
- PHOT_AUTOPARAMS = 2.5, 3.5
- BACK_SIZE = 128

Other values were kept to their default parameters and were not varied during the optimisation. For information regarding each parameter, please refer to the SExtractor documentation. SExtractor additionally provides the option to apply several types of filters to an image, in order to smooth out the image and make detections easier (Casey, 2006). The so-called 'mexhat' filters are particularly applicable to DF2, as the core of the diffuse galaxy constitutes a crowded field. This type of filter is designed to aid in detecting objects within such crowded fields, and is tuned specifically towards detecting objects between FWHMs of 1.5 to 5 pixels.

SExtractor creates user-specified output catalogs containing relevant parameters. For this analysis, the following parameters were retrieved by SExtractor:

- NUMBER
- FLUX_ISO
- FLUXERR_ISO
- MAG_ISO
- MAGERR_ISO
- MAG_APER
- MAGERR_APER
- MAG_AUTO
- MAGERR_AUTO
- X_IMAGE
- Y_IMAGE
- ALPHA_J2000
- DELTA_J2000
- FWHM_IMAGE
- FWHM_WORLD
- ELLIPTICITY
- FLAGS
- CLASS_STAR

After obtaining one output catalog for each filter using SExtractor under its optimal parameters, the catalogs were cross-matched to exclude any uncorroborated detections. The final master catalog, containing only the matched sources, consists of 15870 detections. In order to identify the globular clusters, a selection based on their expected colours and sizes were made.

2.3 Photometric selection

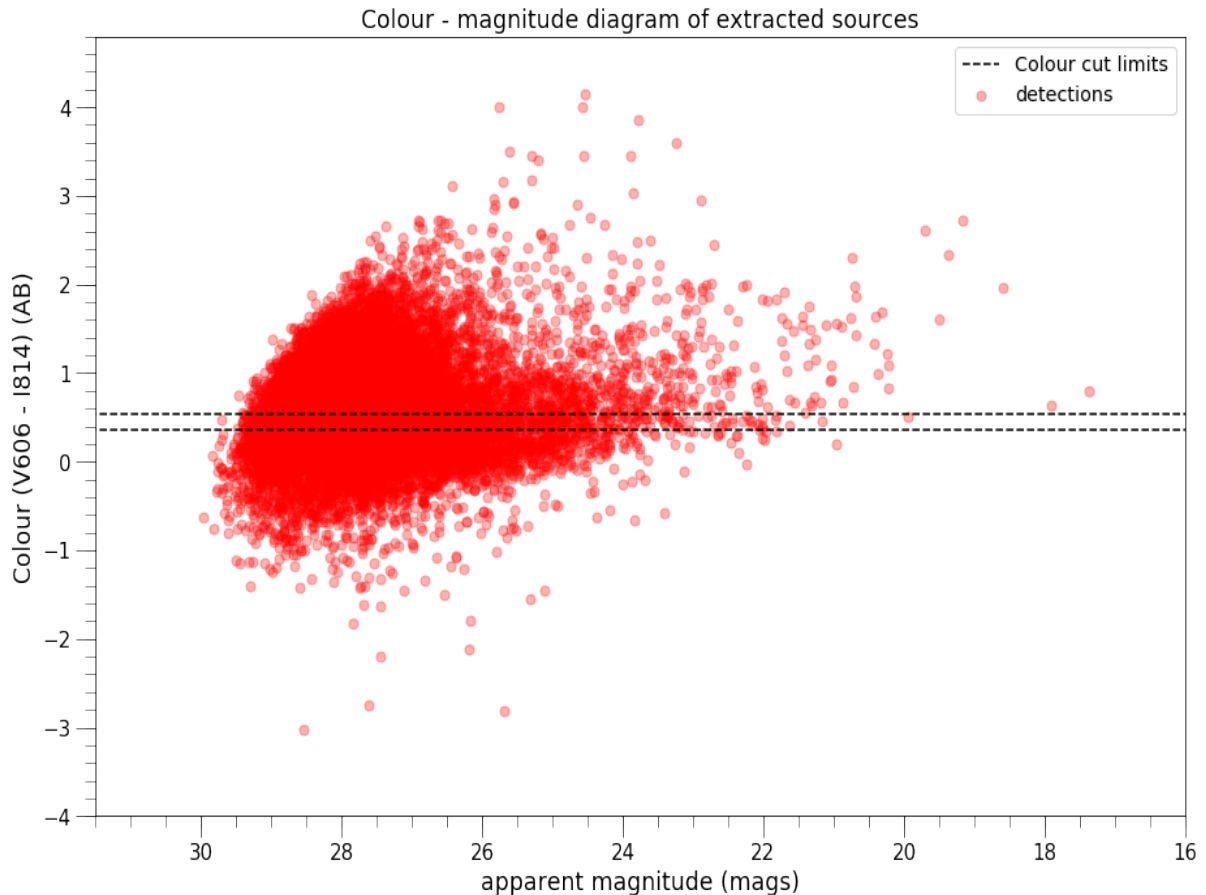


Figure 1: Colour-magnitude diagram of the matched detections. Colours are listed via their AB-magnitude system designations. Colour cut limits are indicated in the plot, at $V_{606} - I_{814} = [0.37, 0.52]$. Colour cut limits were computed from SExtractor measurements of confirmed globular clusters. Unconfirmed globular clusters are expected to fall within this colour range.

Following a similar methodology to the one outlined by Shen et al. (2021b), confirmed globular clusters associated with DF2 were highlighted in the master catalog so that their measured photometric properties could be used. First a $V_{606} - I_{814}$ colour selection was made based on the magnitude data of the globular clusters adhering to the following relation: $\langle V_{606} - I_{814} \rangle \pm 3\sigma$, with σ being the standard deviation of the colours. This selection gives a colour range of $[0.37, 0.52]$. Although Shen et al. (2021b) used a 2σ cut for their colour selection, here we have extended the cut to 3σ to accommodate the deeper data. This colour selection includes all globular clusters from the previous catalog. It can be seen from the colour-magnitude diagram in figure 1 that the colour selection greatly reduces the amount of candidates; of the original 15870 sources, 1593 remain. Figure 2 shows the selection in much more detail, and shows how all spectroscopically confirmed globular clusters from previous works on DF2 are included within the colour cut. From the selected sources, a subsequent size selection was made from the FWHM of each source in pixels. We took a threshold of 4.7 pixels as the maximum value. This value is based on research by Shen et al. (2021b), who took a FWHM cut according to $\langle FWHM \rangle \pm 2.5\sigma_{FWHM} = 4.7$. To make sure that no confirmed globular clusters are excluded from the size cut, we use this value.

The result of applying this cut on the colour-selected detections is shown in figure 3

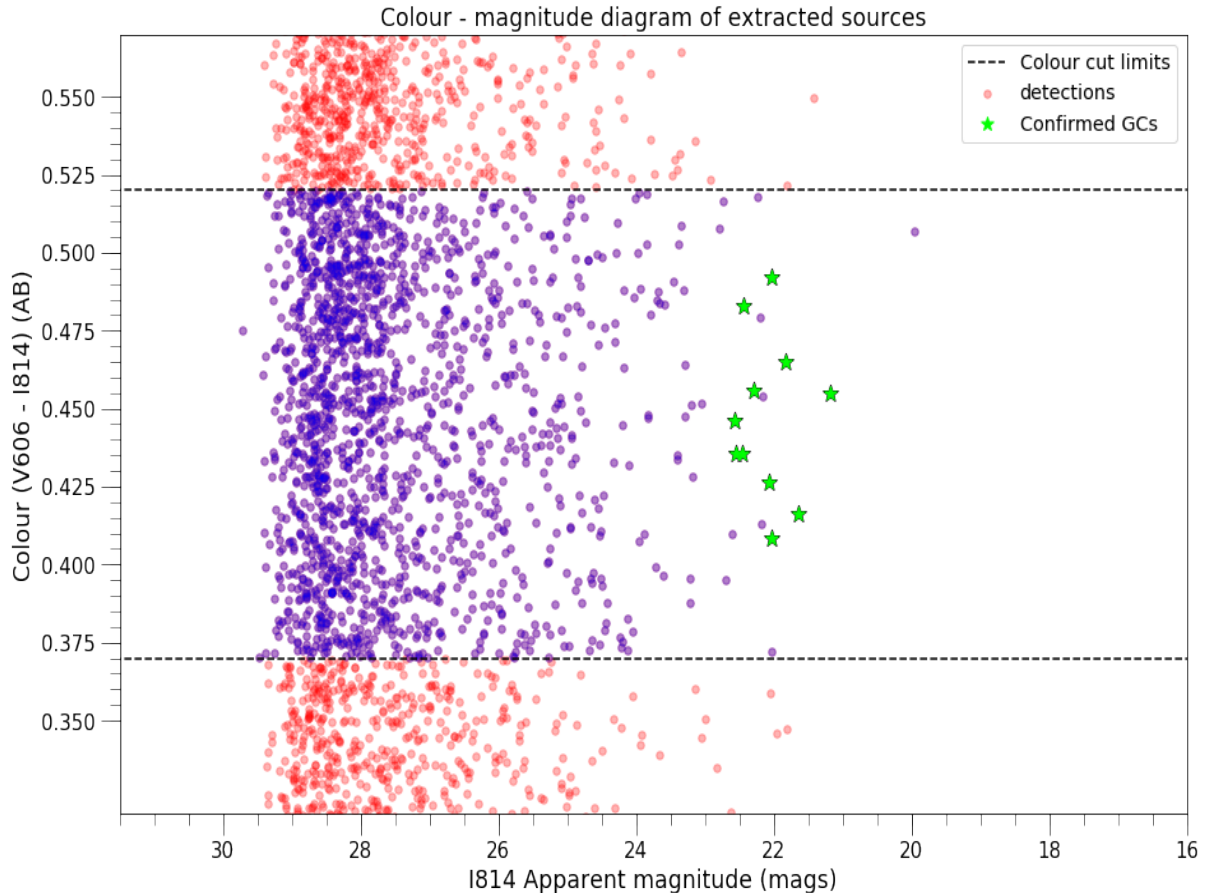


Figure 2: Colour-magnitude diagram of the matched detections, zoomed in on the region between the colour cut limits as outlined in figure 1. A subset of the detections was made, consisting of 1593 sources out of the original 15870.

After the size selection, there are 827 sources remaining within the set criteria. Although many of these sources are expected to be faint background objects and stars, some may constitute globular clusters that have not been confirmed yet, and the previously documented globular clusters all lie within the selection. From here, a statistical background subtraction process is applied. A circular aperture of n half-light (or effective) radii is made around DF2's centre, as seen in figure 5. Taking the half-light radius of DF2 as 2.2 Kpc as according to van Dokkum et al. (2018b), we convert this to a pixel value by computing the angle that DF2 subtends across the sky (assuming a distance of 20 Mpc) in arcsec. We then convert this to pixels using the ACS pixel size of 0.05. (Saifollahi et al., 2022) Magnitude histograms are made for sources outside and inside the aperture, and normalized by area through the following relation to approximate a background magnitude:

$$M_{bg} = \frac{H_{ext} \cdot A_{int}}{A_{ext}}$$

This background magnitude is subtracted from the interior magnitude histogram to provide the final GCLF. This process is performed for $n = 2, 3$ and 4 in order to examine the difference this makes for the background estimation. It should be noted that several confirmed globular

clusters lie outside the aperture for $n = 2$ and $n = 3$, meaning the background is overestimated in those scenarios.

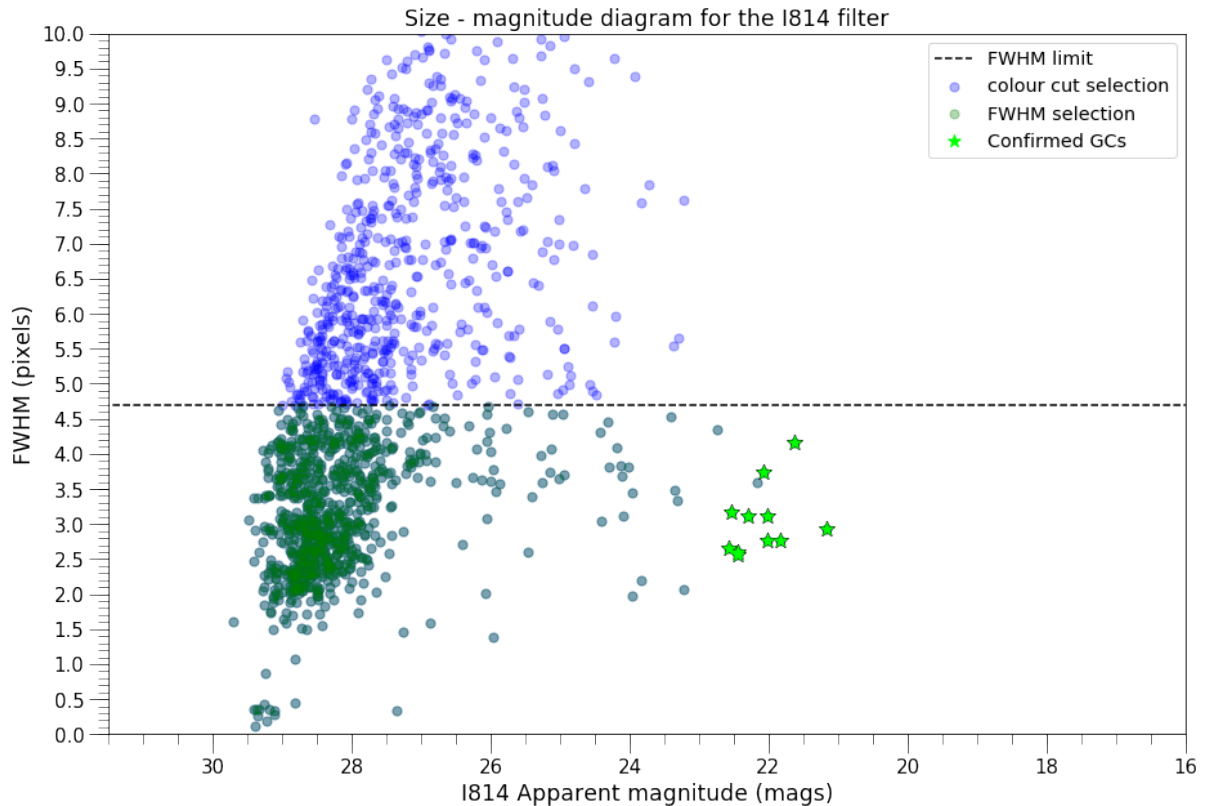


Figure 3: Size-magnitude diagram of the colour-selected detections. The dashed line represents our FWHM cut at 4.7 pixels. All confirmed globular clusters (lime stars) fall underneath this size cut. The figure is capped off at $FWHM = 10$, as the few sources above this size limit are not important to the further background computation. The final cut (green) numbers 827 sources.

2.4 Errors

Though there may be other factors of uncertainty in the assumptions made throughout this work (please refer to the discussion section for more details), the majority of the error bars in the magnitude histograms arise from Poisson noise. Poisson noise, or shot noise, arises due to the quantized nature of light. As light consists of a discrete number of photons, fluctuations in the amount of photons hitting a detector occur naturally. If a source is sufficiently bright or close, many billions of photons may hit a detector at any given time and the minor fluctuations are negligible. If only a small number of photons hit the detector per unit time, as is the case with extremely distant or faint sources, the random fluctuations become significant. These fluctuations may be described by a Poisson distribution. The ratio of signal to photon noise is equal to \sqrt{N} , with N the number of photons captured. As such, poisson noise is relatively weaker at higher signal levels (Hasinoff, 2012).

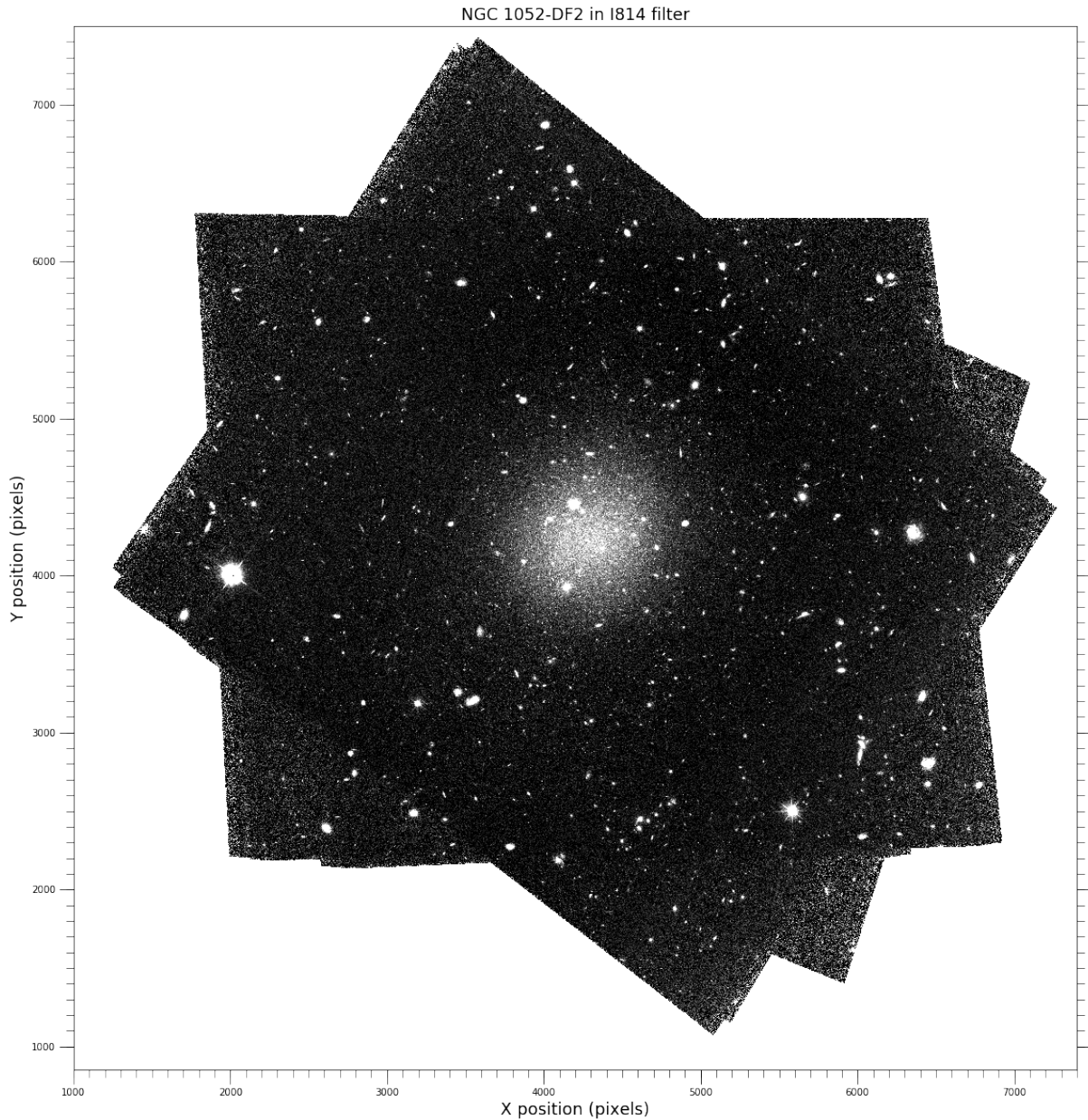


Figure 4: NGC-1052 DF2 as seen in the I_{814} filter. The x and y positions of each pixel in the image were plotted against each other to form the image.

2.5 Apertures

It may be noted from figures [4](#) and [5](#) that the images of DF2 appear cut and jagged around their corners. The cause for this is that the observatory applies a slight rotation in each orbit, in order to capture data on DF2 under slightly different orientations. This has the benefit that any possible bad pixels or bad detections are not stacked up in one single pixel, and so can be smoothed out during data reduction. The images were, as previously mentioned, stacked up to form these final images, explaining the seemingly erratic aperture shape.

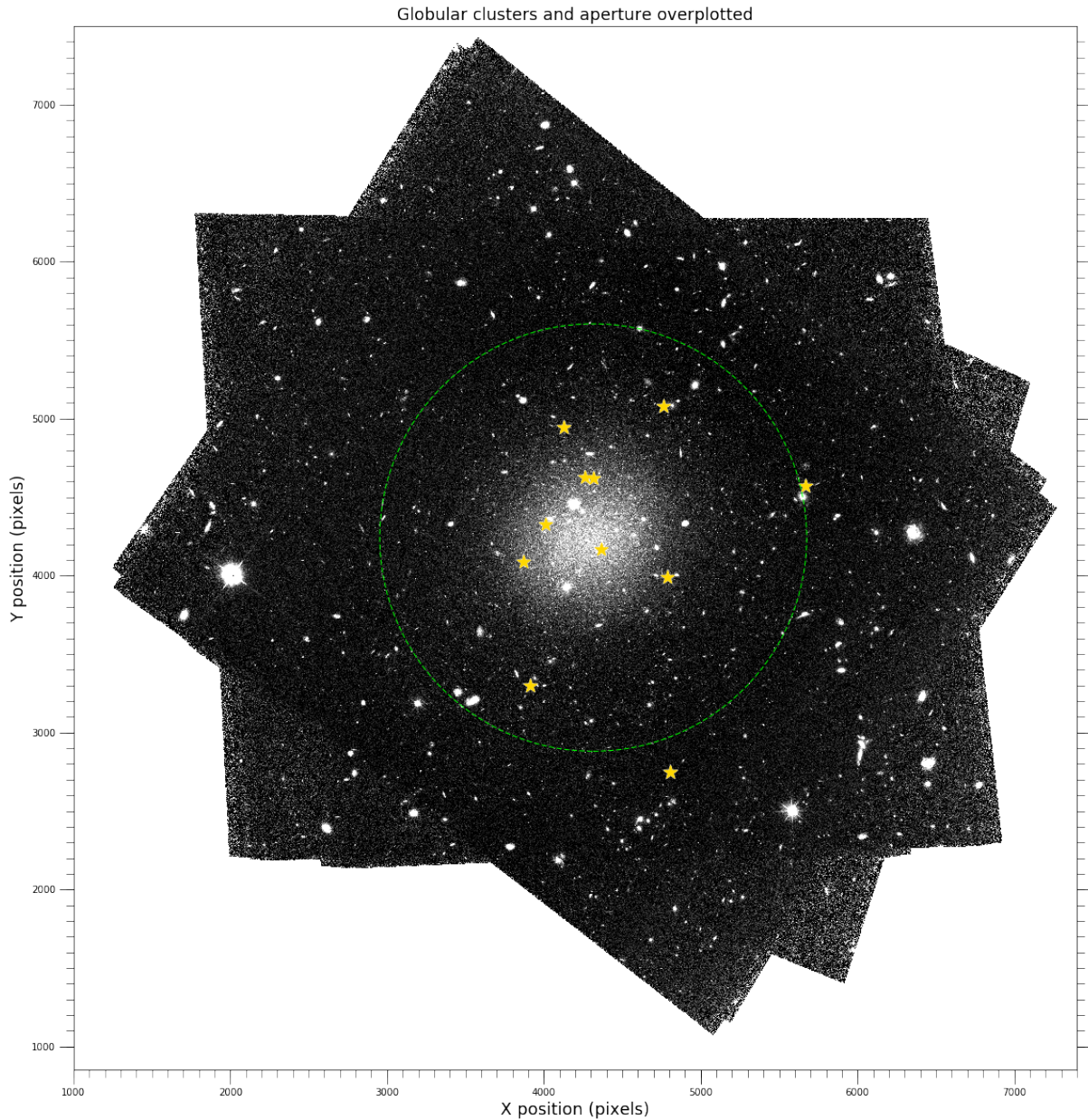


Figure 5: NGC-1052 DF2 in the I_{814} filter, using x / y pixel position on the axes. Overplotted in star markers are globular clusters spectroscopically confirmed by previous works. The green dotted circle represents three half-light radii R_e , used in the background subtraction process. Sources external to the circle are compiled to an external luminosity function which is normalized and subtracted from the GCLF from inside the aperture. Note that since one confirmed globular cluster lies outside the aperture, the background may be slightly overestimated for this case, and even more so for $2R_e$

3 Results

3.1 Luminosity Functions

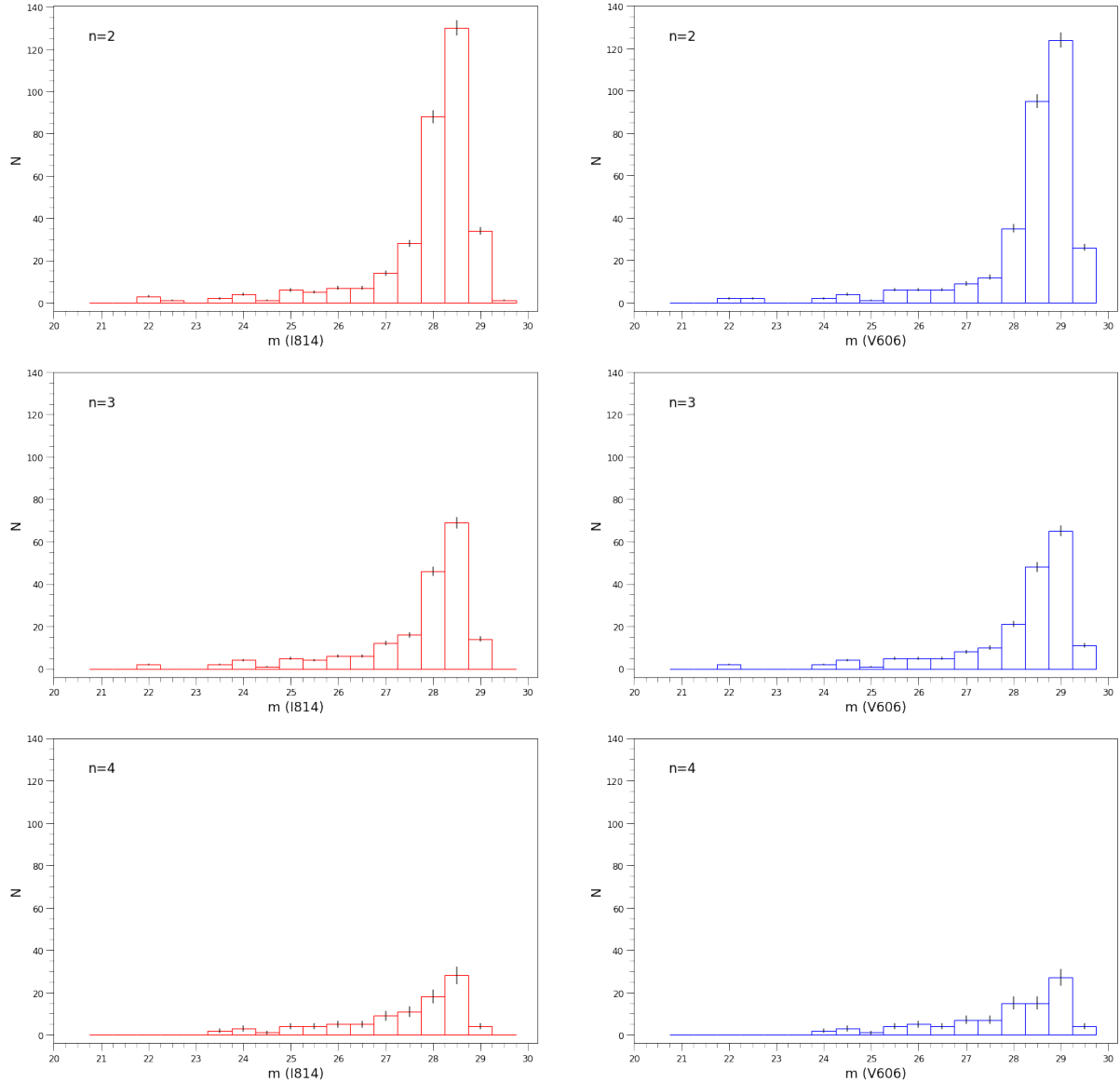


Figure 6: Magnitude histograms of all sources exterior to nR_e , R_e being DF2's effective radius. Plotted are exterior histograms for $n = 2$, $n = 3$ and $n = 4$ in the I_{814} (red) and V_{606} (blue) filters. The symmetric error bars arise due to the Poisson Errors of each bin. Note that for $n \neq 4$, several globular clusters are excluded in the exterior sample, which can be seen around $m \approx 22$

The matched catalog was taken through the described selection cuts, leaving 827 sources. This selection thus includes all sources with colours in the range $[0.37, 0.52]$ and with seeing FWHMs smaller than 4.7. A significant number of sources, particularly within the confines of DF2, are thought to be red giants and supergiants, based on their colours, ellipticities and small FWHMs. The background subtraction process was carried out several times, for two, three and four times

the effective radii. The completeness of the globular clusters within the circular aperture are 63% under $2R_e$, 82% under $3R_e$ and 100% under $4R_e$, meaning the background does not include any of the globular clusters for a background subtraction using $4R_e$. The area of the full image as well as the aperture areas were computed, giving $\frac{A_{ext}}{A_{int}} = 9.22, 3.55$ and 1.57 for $2R_e, 3R_e$ and $4R_e$, respectively. No uncertainties are taken into account for these ratios, as all areas are computed in units of pixels, and the error in the circular aperture is at most equal to the circumference of the aperture. The difference in result due to the circumference is negligible. Similar to the work by Shen et al. (2021b), we count objects within the magnitude range $M_V = -5$ to -11 in the background subtracted GCLF's. They range from $N_{GC} = 12 \pm 5$ at least to $N_{GC} = 14 \pm 6$ at most, correspondent with the I_{814} filter for $3R_e$ and the I_{814} filter for $4R_e$ respectively. The errors in these results, as well as in the histograms and GCLFs, arise purely from the Poisson-distributed shot error of the detectors.

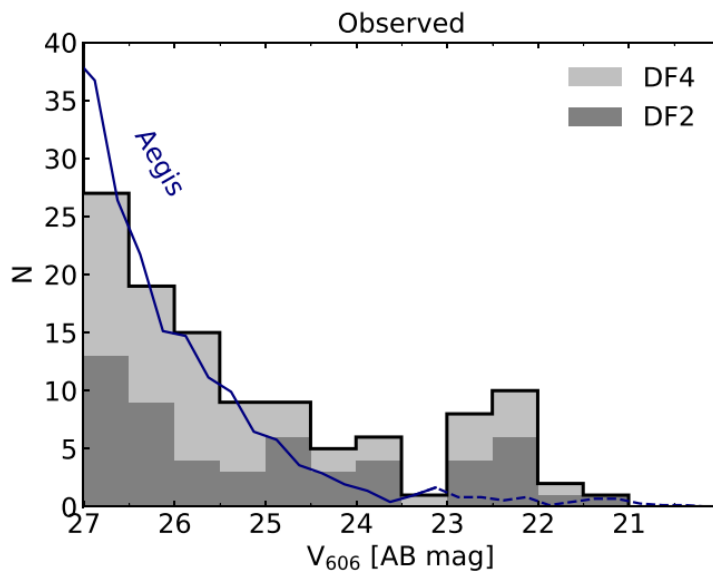


Figure 7: Image taken from Shen et al. (2021b), showing the observed, uncorrected luminosity function of their combined DF2 + DF4 dataset. The blue lines represents AEGIS data of objects with similar colours and sizes to the confirmed globular clusters, which Shen et al. (2021b) used as their background.

The histograms of exterior sources (figure 6) show a steadily increasing frequency of sources with fainter magnitudes, eventually spiking around a magnitude of ≈ 27 , where faint sources dominate the bins. A comparison can be made to the background used by Shen et al. (2021b), which is shown in figure 7. As can be seen from figure 6, several bright globular clusters are included in the histograms under $2 - 3R_e$, as not all globular clusters fall within the circular aperture in these cases. Note the steady decrease of sources as the aperture for background subtraction increases, and the relatively larger error bars for the $4R_e$ case. Since Poisson errors scale with the root of the sample size, the errors are most significant in the $4R_e$ case.

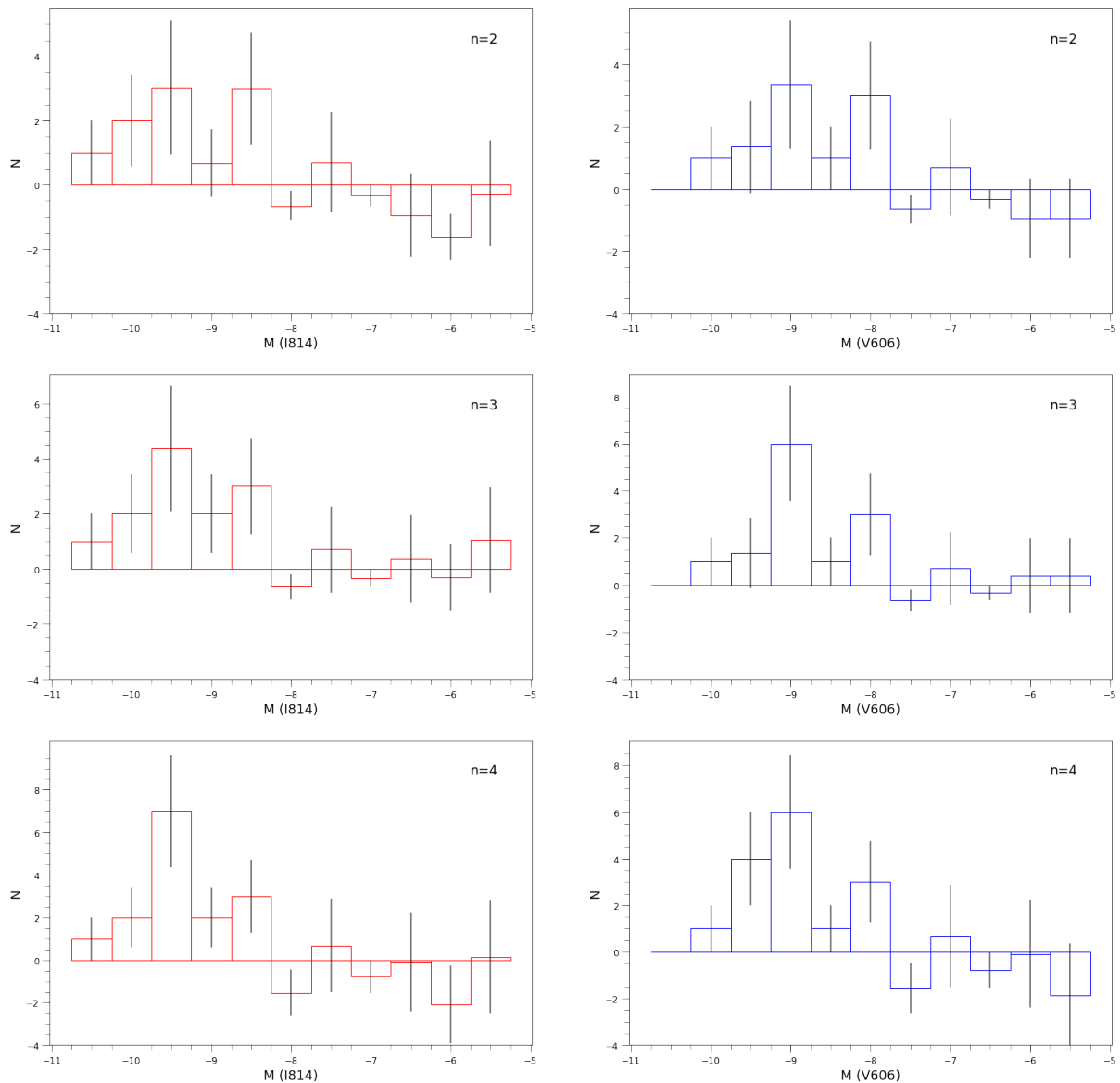


Figure 8: GCLF of DF2’s globular clusters in the I_{814} (red) and V_{606} (blue) filters. The luminosity functions are background corrected through a statistical subtraction process with circular apertures of radius nR_e , with R_e being the effective radius of DF2. Each GCLF shows a clear peak around $M = -9.5$. In none of the cases is there a clear second peak around $M = -7.5$.

The background-subtracted Globular Cluster Luminosity Functions were made for both filters under all three effective radii, with the results being presented in figure 8. In order to make a direct comparison to the works by van Dokkum et al. (2018a) and Shen et al. (2021b), we plot the absolute GCLFs by assuming a distance of 20 Mpc to DF2, which is consistent with a distance modulus of -31.5 . Plotting the absolute magnitude GCLF in figure 8, it is apparent that there is a clear peak around $M_V = -9$, as stated by the previous works. We however see no clear secondary peak around the canonical value of $M_V = -7.5$, unlike the work by Shen et al. (2021b). The absence of such a secondary peak is absent in both filters and under all three cases of background subtraction, as seen in figure 8, but is most clearly seen in the cases of $4R_e$.

3.2 Gaussian modeling

In order to test the hypothesis that the GCLFs of DF2 adhere to a standard Gaussian-like luminosity function, we fit a gaussian function with a mean $\mu \approx -9$, standard deviation $\sigma = 1$ and scaling A . The initial guess for standard deviation and scaling factor A were taken arbitrarily, as the fitting function rapidly converges to a suitable value regardless. Such Gaussian functions with three degrees of freedom were fitted to all GCLFs, with the fit for V_{606} under three effective radii being shown in figure 9. The poisson errors for each bin are taken into account during the fitting. The best fit is a Gaussian with a mean of $\mu = -8.8$, $\sigma = 0.76$. A reduced χ^2 test is performed on each fit, with the best fit having a χ^2 statistic of 3.45. This would indicate that the fit does not model the data very well. A second fit using a bimodal fit with a fixed second mode at $\mu_2 = -7.5$ was also performed, in accordance with the methodology of Shen et al. (2021b). This model gives, at best, a χ^2 statistic of 20.8, indicating that the single mode Gaussian fit is at the very least a more suitable model for the GCLF.

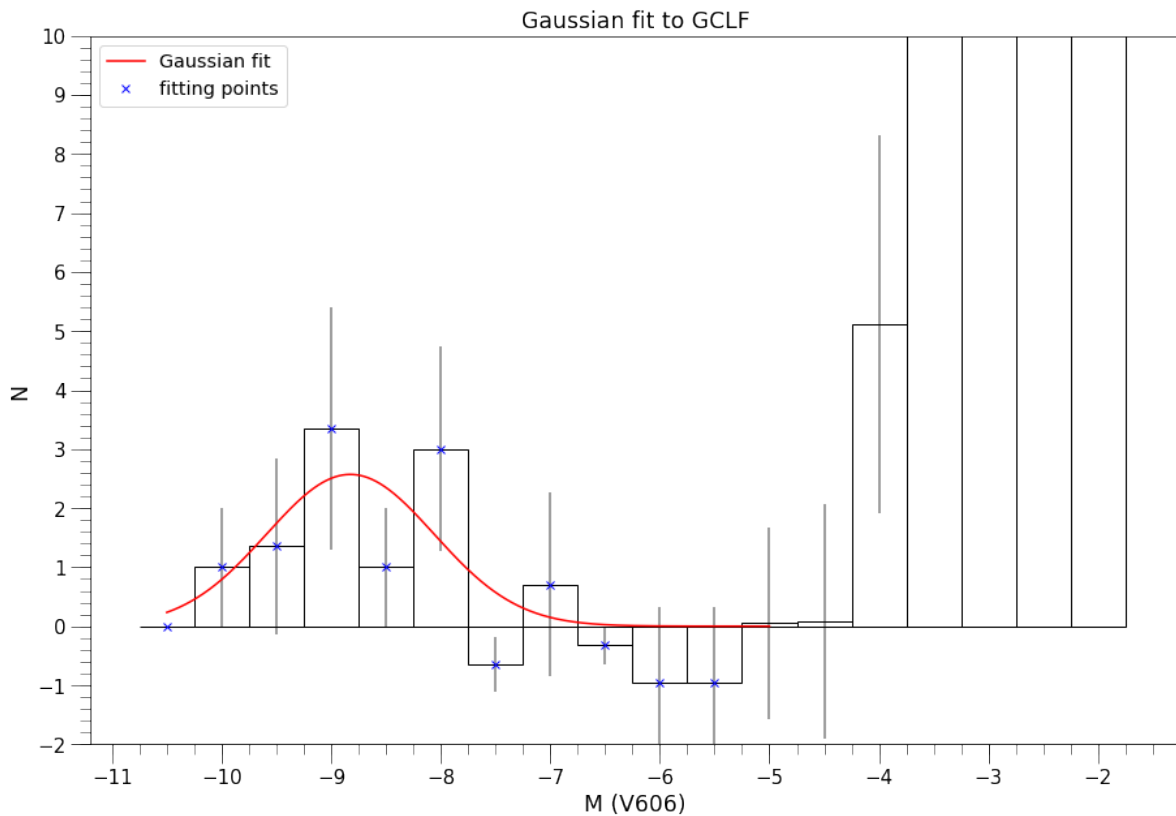


Figure 9: GCLF in the V_{606} filter, background corrected using a $3R_e$ aperture. A gaussian fit with estimated parameters $\mu = -9$, $\sigma = 1.5$ has been fitted to the bin points marked in blue, in order to test the single mode Gaussian hypothesis. The fit to the data is poor, with a χ^2 statistic of 3.45.

4 Discussion

As was stated in the introduction, this thesis aimed to investigate the bimodality of the GCLF of DF2 as was purported by Shen et al. (2021b). In this section we will discuss the methodology of this work critically, and review any assumptions made on their validity. We will discuss the

discrepancy in the result of this thesis and the results of the work by Shen et al. (2021b), particularly the means by which the background was computed in both works. Several suggestions for follow up research into DF2 and its globular cluster system will also be discussed.

A significant amount of time went in to optimising SExtractor to good performance in the crowded field of DF2. The process was done manually, and no machine learning or automation was used. It is therefore likely that there are superior setups that would perform better, qualitatively, quantitatively or both, than the one ultimately used in this thesis. A follow-up study related to this thesis might benefit from a review of the SExtractor configuration.

As this thesis aims to investigate the purported bimodality of the GCLF of DF2's globular cluster system, care was taken to follow the methodology by Shen et al. (2021b) closely in order to make a fair comparison. Two major differences may be pointed out in the methodologies: the deeper data of this thesis and the difference in background subtraction. In this thesis, we applied a statistical background subtraction process based on the magnitudes of sources after selection, with a normalization to unit area. The previous work instead used the All-wavelength Extended Growth Strip International Survey (AEGIS) field, from the 2014 Hubble Space Telescope data release. Aegis is a multiwavelength sky survey, formed up from observations by the Chandra, GALEX, Hubble, Keck, CFHT, MMT, Subaru, Palomar, Spitzer and VLA telescopes. Shen et al. (2021b) used sources from the AEGIS catalog, applied similar selection cuts and constructed a luminosity function, which was then statistically subtracted from their GCLF as a background. The major difference between the two methods is that AEGIS sources are distributed across the whole sky, and are not local to DF2, while our background subtraction method is. It is difficult to qualitatively assert which method of background correction is better. The previous paper did not motivate explicitly why background subtraction using AEGIS data was chosen. In this thesis we utilized the local background subtraction since the data on DF2 is very deep, allowing the background in the image to be determined to a higher degree of accuracy than before.

The peak of the luminosity function is of course a distance-dependant quality, since the apparent magnitudes cannot be converted to absolute magnitudes without a distance modulus. It should also be noted that we use a distance of 20 Mpc in the computation of the half-light radius in pixel values for the background subtraction, making our subtraction distance-dependant. If we instead utilize a distance of 13.4 Mpc as cited by Trujillo et al. (2019), the half-light radius would be 49% larger. From looking at figure 6 we can infer that this would imply a smaller background. Given that we perform a near-direct comparison to previous works which also adopted this distance, this should not be considered significant to the overall result, particularly since the presence of a second peak within the GCLF is not distance dependant. The measured number of objects within magnitude ranges from -5 to -11 is bigger than the number of spectroscopically confirmed GCs (12 ± 5 candidates compared to 11 confirmed GCs), and we cannot say for certainty that the excess objects counted are truly globular clusters. It is likely that they are foreground stars of similar colour or luminous background objects.

In computing the χ^2 statistics for all fits, one reason for the poor quality of the fits is the small amount of datapoints. A luminosity function with more sources may follow the expected Gaussian behaviour more closely, as seen with the Milky Way's GCLF which contains approximately 157 sources. (Frommert, 2011) (Harris, 1996) On top of this, it should be pointed out that the bimodal fit is biased to lower values as the fit contains more degrees of freedom. This supports the argument that the single mode Gaussian fit is more suited to DF2's GCLF, as its χ^2 statistic is lower than that of the bimodal fit despite them being on unequal footing. To corroborate

this, more statistical tests may be performed on the fits, such as the Kolmogorov-Smirnov (KS) statistic or a Shapiro-Wilk test. Both test the hypothesis if a given set of observations match a given distribution, and can be used in this context.

For future studies into the purported bimodality of DF2's GCLF, we would suggest the following improvements to this work. Firstly, a more direct comparison to the results of Shen et al. (2021b) can be done if an identical background subtraction method is used on the deeper data. This would allow us to verify whether the difference in result arises purely from the different backgrounds. Additionally, there may be benefits to running an optimization program on SExtractor to find a superior configuration than the one used in this thesis. It should also be noted that Shen et al. (2021b) used a combined sample of globular clusters from DF2 and a similar galaxy, NGC-1052 DF4. As such, their sample size is larger, improving the quality of their models by nature of having more fittable datapoints. Forming a similar combined sample from globular cluster data of DF4 may allow statistical tests like those used in this report to be carried out with a higher degree of accuracy. It may also be argued that the difference between our result and that of the previous work arises not just from the background subtraction, but from this combination of samples. If this is the case, there may be no bimodality in the GCLF of either galaxy at all, it simply being an apparent result from the combination of two different datasets.

5 Conclusion

This thesis used extremely deep HST-ACS data to investigate the globular cluster system of the seemingly anomalous galaxy NGC-1052 DF2. By using Source Extractor and several selection cuts, some 800 sources were used to form the Globular Cluster Luminosity Function. The results of the analysis are as follows:

- We find $N_{GC} = 12 \pm 5$ at least and $N_{GC} = 14 \pm 6$ at most, though these values are misleading to the true number of globular clusters in association with DF2.
- We observe clear peaks in the GCLF of DF2 around -9 for all filters and all background subtraction cases, taking a distance modulus of -31.5 in accordance with a distance of 20 Mpc.
- We observe no evidence of a 'second peak' around $M_V = -7.5$, unlike Shen et al. (2021b).
- Our reduced χ^2 test on Gaussian and bimodal Gaussian models yield values of 3.45 and 20.8 respectively, indicating that the Gaussian fit is far better than the bimodal fit.

Though the methodology of the previous paper has been followed closely in order to make a direct comparison, the differences in result could arise from the different background subtraction methods that were used by the two works. Direct comparison with the background subtraction method of the previous work was not possible since we do not possess their data.

Though it may seem like DF2 remains anomalous given the brighter peak of the GCLF, it should again be noted that a distance of 20 Mpc was adopted in this project, giving an absolute magnitude around -9 for the peak of the luminosity function. The real distance to DF2 is still a debated subject, and a distance of 13.4 Mpc would instead shift the peak to lie around the canonical value of -7.5 . As our aim was to investigate the appearance of a secondary peak, the distance we take to DF2 is not too relevant, and the mystery behind its true distance will

need to be investigated by other studies. If the conservative distance of 13.4 Mpc is correct, it would leave plenty of room for a dark matter halo in DF2 and its GCLF would shift towards the universal values. It would imply that DF2 is a standard UDG with no apparent anomalies. There remains the possibility that the larger distances of 20 Mpc assumed by [van Dokkum et al. \(2018b\)](#) or even the revised 22.1 ± 1.2 Mpc as found by [Shen et al. \(2021a\)](#) are correct. This would imply that DF2 is extraordinary, and challenges current models on the formation of dwarf galaxies and the luminosities of globular clusters. It will be highly interesting to see how the debate regarding this galaxy develops over the next decade.

6 References

References

- Aladin sky atlas, 2005. URL <https://aladin.u-strasbg.fr/>.
- SExtractor user manual — sExtractor 2.24.2 documentation, 2013. URL <https://sextractor.readthedocs.io/en/latest/>.
- A. Barbara. Hst proposal search, 2019. URL https://archive.stsci.edu/proposal_search.php?id=15851&mission=hst.
- M. A. Beasley. Globular cluster systems and galaxy formation. *arXiv:2003.04093 [astro-ph]*, 1:245–277, 2020. doi: 10.1007/978-3-030-38509-5_9. URL <https://arxiv.org/abs/2003.04093>.
- B. Binggeli, A. Sandage, and G. A. Tammann. Studies of the virgo cluster. ii - a catalog of 2096 galaxies in the virgo cluster area. v - luminosity functions of virgo cluster galaxies. *The Astronomical Journal*, 90:1681, 09 1985. doi: 10.1086/113874.
- C. Casey. Optimizing sExtractor parameters for subaru macs fields, 2006. URL <http://www.ifa.hawaii.edu/reu/reu2006/casey.pdf>.
- P. v. Dokkum, R. Abraham, J. Brodie, C. Conroy, S. Danieli, A. Merritt, L. Mowla, A. Romanowsky, and J. Zhang. A high stellar velocity dispersion and 100 globular clusters for the ultra-diffuse galaxy dragonfly 44. *The Astrophysical Journal*, 828:L6, 08 2016. doi: 10.3847/2041-8205/828/1/L6.
- P.-A. Duc, S. Paudel, R. M. McDermid, J.-C. Cuillandre, P. Serra, F. Bournaud, M. Cappellari, and E. Emsellem. Identification of old tidal dwarfs near early-type galaxies from deep imaging and hi observations. *Monthly Notices of the Royal Astronomical Society*, 440:1458–1469, 03 2014. doi: 10.1093/mnras/stu330.
- H. Frommert. Milky way globular clusters, 2011. URL <http://spider.seds.org/spider/MWGC/mwgc.html#harris>.
- W. E. Harris. Globular cluster systems in galaxies beyond the local group. *Annual Review of Astronomy and Astrophysics*, 29:543–579, 09 1991. doi: 10.1146/annurev.aa.29.090191.002551.
- W. E. Harris. A catalog of parameters for globular clusters in the milky way. *The Astronomical Journal*, 112:1487, 10 1996. doi: 10.1086/118116.

- S. Hasinoff. Photon , poisson noise, 2012. URL <https://people.csail.mit.edu/hasinoff/pubs/hasinoff-photon-2012-preprint.pdf>.
- M. Montes, I. Trujillo, R. Infante-Sainz, M. Monelli, and A. S. Borlaff. A disk and no signatures of tidal distortion in the galaxy “lacking” dark matter ngc 1052-df2. *The Astrophysical Journal*, 919:56, 09 2021. doi: 10.3847/1538-4357/ac0d55.
- O. Müller, R. M. Rich, J. Román, M. K. Yıldız, M. Bílek, P.-A. Duc, J. Fensch, I. Trujillo, and A. Koch. A tidal tale: detection of several stellar streams in the environment of ngc 1052. *Astronomy Astrophysics*, 624:L6, 04 2019. doi: 10.1051/0004-6361/201935463.
- G. Ogiya, F. C. van den Bosch, and A. Burkert. On the tidal formation of dark matter-deficient galaxies. *Monthly Notices of the Royal Astronomical Society*, 510:2724–2739, 12 2021. doi: 10.1093/mnras/stab3658.
- M. Rejkuba. Globular cluster luminosity function as distance indicator. *Astrophysics and Space Science*, 341:195–206, 01 2012. doi: 10.1007/s10509-012-0986-9.
- J. Román, A. Castilla, and J. Pascual-Granado. Discovery and analysis of low-surface-brightness galaxies in the environment of ngc 1052. *Astronomy & Astrophysics*, 656:A44, 12 2021. doi: 10.1051/0004-6361/202142161.
- T. Saifollahi. *Understanding the Extreme Classes of Dwarf Galaxies*. PhD thesis, 2022.
- T. Saifollahi, D. Zaritsky, I. Trujillo, R. F. Peletier, J. H. Knapen, N. Amorisco, M. A. Beasley, and R. Donnerstein. Implications for galaxy formation models from observations of globular clusters around ultradiffuse galaxies. *Monthly Notices of the Royal Astronomical Society*, 511: 4633–4659, 02 2022. doi: 10.1093/mnras/stac328.
- Z. Shen, S. Danieli, P. van Dokkum, R. Abraham, J. P. Brodie, C. Conroy, A. E. Dolphin, A. J. Romanowsky, J. M. Diederik Kruijssen, and D. Dutta Chowdhury. A tip of the red giant branch distance of 22.1 ± 1.2 mpc to the dark matter deficient galaxy ngc 1052-df2 from 40 orbits of hubble space telescope imaging. *The Astrophysical Journal Letters*, 914:L12, 06 2021a. doi: 10.3847/2041-8213/ac0335.
- Z. Shen, P. van Dokkum, and S. Danieli. A complex luminosity function for the anomalous globular clusters in ngc 1052-df2 and ngc 1052-df4. *The Astrophysical Journal*, 909:179, 03 2021b. doi: 10.3847/1538-4357/abdd29.
- E.-j. Shin, M. Jung, G. Kwon, J.-h. Kim, J. Lee, Y. Jo, and B. K. Oh. Dark matter deficient galaxies produced via high-velocity galaxy collisions in high-resolution numerical simulations. *The Astrophysical Journal*, 899:25, 08 2020. doi: 10.3847/1538-4357/aba434.
- J. Silk. Ultra-diffuse galaxies without dark matter. *Monthly Notices of the Royal Astronomical Society: Letters*, 488:L24–L28, 07 2019. doi: 10.1093/mnrasl/slz090.
- I. Trujillo, M. A. Beasley, A. Borlaff, E. R. Carrasco, A. Di Cintio, M. Filho, M. Monelli, M. Montes, J. Román, T. Ruiz-Lara, J. Sánchez Almeida, D. Valls-Gabaud, and A. Vazdekis. A distance of 13 mpc resolves the claimed anomalies of the galaxy lacking dark matter. *Monthly Notices of the Royal Astronomical Society*, 486:1192–1219, 03 2019. doi: 10.1093/mnras/stz771. URL <https://academic.oup.com/mnras/article/486/1/1192/5380810>.

- P. van Dokkum, R. Abraham, A. J. Romanowsky, J. Brodie, C. Conroy, S. Danieli, D. Lokhorst, A. Merritt, L. Mowla, and J. Zhang. Extensive globular cluster systems associated with ultra diffuse galaxies in the coma cluster. *The Astrophysical Journal*, 844:L11, 07 2017. doi: 10.3847/2041-8213/aa7ca2.
- P. van Dokkum, Y. Cohen, S. Danieli, J. M. D. Kruijssen, A. J. Romanowsky, A. Merritt, R. Abraham, J. Brodie, C. Conroy, D. Lokhorst, L. Mowla, E. O’Sullivan, and J. Zhang. An enigmatic population of luminous globular clusters in a galaxy lacking dark matter. *The Astrophysical Journal*, 856:L30, 03 2018a. doi: 10.3847/2041-8213/aab60b.
- P. van Dokkum, S. Danieli, Y. Cohen, A. Merritt, A. J. Romanowsky, R. Abraham, J. Brodie, C. Conroy, D. Lokhorst, L. Mowla, E. O’Sullivan, and J. Zhang. A galaxy lacking dark matter. *Nature*, 555:629–632, 03 2018b. doi: 10.1038/nature25767. URL <https://www.nature.com/articles/nature25767>.
- P. van Dokkum, S. Danieli, R. Abraham, C. Conroy, and A. J. Romanowsky. A second galaxy missing dark matter in the ngc 1052 group. *The Astrophysical Journal*, 874:L5, 03 2019. doi: 10.3847/2041-8213/ab0d92.
- P. G. van Dokkum, R. Abraham, A. Merritt, J. Zhang, M. Geha, and C. Conroy. Forty-seven milky way-sized, extremely diffuse galaxies in the coma cluster. *The Astrophysical Journal*, 798:L45, 01 2015. doi: 10.1088/2041-8205/798/2/145.

7 Appendix: Python Code

